

Preparation and characterization of LiTi_2O_4 anode material synthesized by one-step solid-state reaction

Jianwen Yang · Jiang Zhao · Yongzhen Chen · Yanwei Li

Received: 2 October 2009 / Revised: 30 November 2009 / Accepted: 31 January 2010 / Published online: 25 February 2010
© Springer-Verlag 2010

Abstract LiTi_2O_4 anode material for lithium-ion battery has been prepared by a novel one-step solid-state reaction method using Li_2CO_3 , TiO_2 , and carbon black as raw materials. X-ray diffraction, scanning electron microscopy, energy-dispersive spectrometry, and the determination of electrochemical properties show that the single phase of LiTi_2O_4 with spinel crystal structure is formed at 850°C by this new method, and the lattice parameter is about 8.392\AA . The primary particle size of the LiTi_2O_4 powder is about $0.5\text{--}1.0\ \mu\text{m}$ and its morphology is similar to a sphere. The lithium ion insertion voltage of LiTi_2O_4 anode material is about 1.50 V versus lithium metal, the initial discharge capacity is about $133.6\ \text{mAh g}^{-1}$, the charge–discharge voltage plateau is very flat, and no solid electrolyte interface film is formed when working potential is more than 1.0 V. The reaction reversibility and the cycling stability are excellent, and the high rate performance is good.

Keywords LiTi_2O_4 · One-step solid-state reaction · Anode material · Lithium-ion battery · Characterization

Introduction

In recent years, high-performance lithium ion batteries that are safety, have long life, low cost, and high-power, have

J. Yang (✉) · J. Zhao · Y. Chen · Y. Li
College of Chemistry and Bioengineering,
Guilin University of Technology,
Guilin 541004, People's Republic of China
e-mail: yangjw@glite.edu.cn

J. Zhao
Research Institute for Micro/Nanometer Science and Technology,
Shanghai Jiao Tong University,
Shanghai 200030, People's Republic of China

been urgently needed in many applications, such as power tools, electric vehicle, and hybrid electric vehicle. It has led to numerous researches on new types of electrode materials for lithium ion batteries [1]. $\text{Li}_4\text{Ti}_5\text{O}_{12}$ has been intensively studied as one of the promising alternatives for the commercial carbon-based anode materials due to its unique properties. For example, the zero strain insertion property shows good reversibility ($>10,000$ times) and capacity retention [2–4]; the combination of high lithium mobility makes it an adequate anode for high rate battery applications [4–6]; the higher working potential (1.55 V vs. Li^+/Li) without lithium metal depositing during a profound cell discharge makes excellent safety compared to the current carbon anodes [2]. However, the electric conductivity of $\text{Li}_4\text{Ti}_5\text{O}_{12}$ is poor (only $10^{-9}\ \text{S cm}^{-1}$ at 20°C), which limits its high rate and/or low temperature application [7]. LiTi_2O_4 and $\text{Li}_4\text{Ti}_5\text{O}_{12}$ are the end members of the solid solution series $\text{Li}_{1+x}\text{Ti}_{2-x}\text{O}_4$ ($0 \leq x \leq 1/3$), and the two compounds exhibit complete crystal structure and very similar electrochemical properties; furthermore, LiTi_2O_4 anode materials have advantages in electric conductivity (the specific resistance is about $1.8\ \text{m}\Omega\ \text{cm}$ at 20°C) [3, 8, 9], which facilitates high rate performance. Therefore, LiTi_2O_4 is a better promising anode material than $\text{Li}_4\text{Ti}_5\text{O}_{12}$. However, synthesis of pure phase LiTi_2O_4 is much more difficult than that of $\text{Li}_4\text{Ti}_5\text{O}_{12}$ because Li^+ in reactants is easy to evaporate and the Ti^{3+} is easily oxidized during a synthesis reaction, so this kind of compound has usually been prepared at a high reaction temperature by two steps and by using a vacuum system ($(3\text{--}4)\times 10^{-7}\text{ Torr}$) [10–12]. In the two-step method, active intermediates (such as Ti_2O_3 , $\text{Li}_2\text{Ti}_3\text{O}_7$, $\text{Li}_2\text{Ti}_2\text{O}_5$, TiO etc.) are being synthesized in priority, and then the LiTi_2O_4 is synthesized with a kind of intermediate through solid state reaction at high temperature in inert atmosphere or vacuum [3, 9, 10, 13–15]. LiTi_2O_4

also can be directly synthesized with Li_2CO_3 and TiO_2 using hydrogen as reducing agent, but it is difficult to control the reaction process [16]. The molten salt electrolytic method has been adopted to prepare LiTi_2O_4 single crystal for superconductivity study [17]. $\text{Li}_{0.5}\text{TiO}_2$ or $\text{Li}_{0.5}\text{Ti}_2\text{O}_4$ are synthesized and then treated at about 500°C in aqueous solution [16, 18, 19]. Nanometer LiTi_2O_4 can be synthesized by hydrothermal method, but it may result in an incomplete reaction and side reaction product [20]. The sol-gel method has also been exploited, but the process is complex [21, 22]. Therefore, it is necessary to develop some novel ways for the synthesis of LiTi_2O_4 . In this paper, a novel one-step solid-state reaction method is proposed for the preparation of LiTi_2O_4 anode material. The microstructure and electrochemical performances of LiTi_2O_4 have been studied, which may pave the way for the application of LiTi_2O_4 in industrial lithium ion batteries.

Experimental

Analytical grade Li_2CO_3 , TiO_2 ($\text{TiO}_2 \geq 98\%$, anatase, and average particle size of 396 nm; from Xilongchem Fac. in China), and carbon black were mixed with the molar ratio of 2.1:8:1.1. Considering the easy evaporation of lithium ions and reduction of Ti^{4+} during reactions, excess of lithium ion and carbon black were added to the reactants. The mixture was transferred in tube furnace and heated at different temperature (800, 850, and 900°C) for 36 h in argon gas. When the synthesized product was cooled naturally to room temperature, it was taken out and grounded. The structure was analyzed by X'Pert PRO X-ray diffractometer (XRD) with $\text{Cu K}\alpha$ radiation ($\lambda=1.5405 \text{ \AA}$). The diffraction peak position was calibrated by silicon with the purity of 99.9%. The particle size and morphology of the products were observed by JSM-5610LV type scanning electron microscopy (SEM) under 15 kV accelerating voltage. The composition of the products was analyzed by INCA350 X-ray energy-dispersive spectrometer (EDS). The lithium content was determined by Optima 2100DV inductive coupled plasma (ICP) spectrometry. The carbon content in the product was determined with TP-2FS carbon and sulfur analyzer.

The cathode was prepared by mixing LiTi_2O_4 , carbon black, and polyvinylidene fluoride (80:10:10, *w/w*), and subsequently, slurry was made with *n*-methyl pyrrolidone. The resulting slurry was coated uniformly onto aluminum foil and dried at 100°C for 10 h in a vacuum dryer. Li metal foil was used as the counter and reference electrodes. The test cells were assembled in an argon-filled glove box (MBraun, USA). The cathode and Li metal foil were separated using Celgard 2400 microporous membrane. A solution of 1 M LiPF_6 in a mixed solvent of ethylene

carbonate/ethylene methyl carbonate/dimethyl carbonate (EC/EMC/DMC) with 1:1:1 volume ratio was used as the electrolyte for all cells. Electrochemical tests were performed using an Autolab electrochemical workstation (Matrohm AG, Switzerland) and PCBT-100-8B battery comprehensive tester (Lixing, China) at room temperature. Cyclic voltammetry (CV) was scanned between 3.0 and 0.8 V with 0.5 mV s⁻¹ sweep rate. Charge and discharge cycling was measured between 3.0 and 0.9 V with 0.2 C, 0.5 C, and 1.0 C constant current densities. Electrochemical impedance spectra was conducted in a frequency range from 100 kHz to 0.001 Hz with 5 mV amplitude.

Results and discussion

Figure 1 shows the XRD patterns of the LiTi_2O_4 powder prepared by one-step solid-state reaction at different temperatures (800, 850, and 900°C) for 36 h in argon gas. When the temperatures are 800 and 900°C, impurity peaks emerge at 27.388°, 41.380°, and 54.283°, indicating that the synthetic product contains a bit of rutile- TiO_2 phase, which may result from the incomplete reactant of TiO_2 at 800°C and the decomposition product of LiTi_2O_4 at 900°C. When the sintering temperature is controlled at 850°C, the product exhibited a single phase, and all the diffraction peaks can be indexed with the face centered cubic spinel structure of LiTi_2O_4 . The lattice constant *a* is about 8.392 Å as calculated by least square method, which is in accordance with the value (*a*=8.400±0.002 Å) as reported by Geng [9]. The crystallite size was estimated by Scherrer formula ($D=0.9\lambda/\beta\cos\theta$) from XRD patterns. The calculated crystallite size is about 35.29 nm. It can be concluded that synthesis temperature is a key factor in obtaining a pure phase LiTi_2O_4 using Li_2CO_3 , TiO_2 , and carbon black as raw materials. The sample contains a bit of carbon black, but its diffraction peaks could not be found out in the patterns, since its content in the product is low (about 0.2% analyzed by TP-2FS carbon analyzer) or showing amorphous state.

Figure 2 shows the EDS spectrum of the LiTi_2O_4 powder sample. The atomic percents of Ti and O in the sample are 33.33% and 66.67%, respectively, and their ratio value is just the same to their molar ratio in LiTi_2O_4 . The weight percentages of Ti and O elements in the sample are 59.95% and 40.05%, respectively, and the sum of them is about 100%. Li element can't be found in the spectrum because it is a light element. The weight percentages of Li element measured by Optima 2100DV ICP is about 4.00% in the sample. Figure 3 is an SEM image of LiTi_2O_4 powder sample. It is observed that the sample is composed of mostly dispersed similar spherical particle and a few

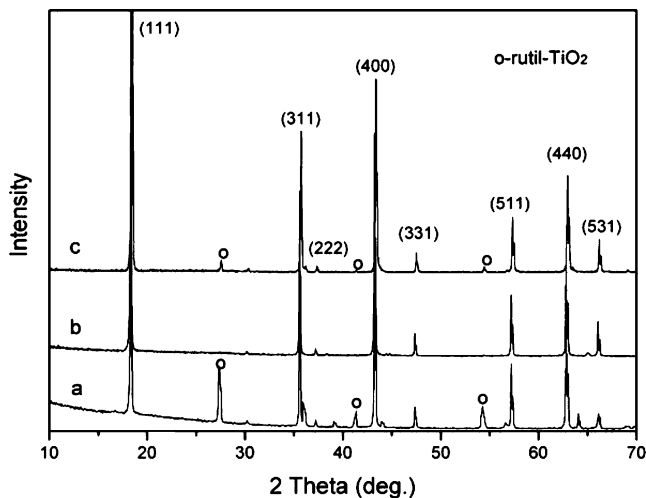


Fig. 1 XRD patterns of LiTi_2O_4 samples obtained at different temperatures: (a) 800°C, (b) 850°C, and (c) 900°C

aggregates. The size of primary powder is uniform and the grain diameter is about 0.5–1.0 μm .

Figure 4 compares the voltammetric behaviors of the LiTi_2O_4 and TiO_2 (anatase) electrodes. It is observed that the peak potentials of lithium ion insertion and de-insertion of TiO_2 are 1.45 and 2.36 V, respectively, and the average potential is about 1.90 V. The peak potentials of lithium ion insertion and de-insertion of LiTi_2O_4 are 1.17 and 1.75 V, respectively, and the average potential is about 1.46 V. The difference between the oxidation peak and reduction peak potential of LiTi_2O_4 sample is 0.58 V, which is smaller than that (0.91 V) of TiO_2 . Furthermore, the current before/after the current peaks of the LiTi_2O_4 electrode changes more quickly than that of TiO_2 during the potential scanning, indicating that the LiTi_2O_4 sample has the better reversibility [23]. No TiO_2 current peak is observed in the CV curve of LiTi_2O_4 , showing that the purity of LiTi_2O_4 sample is very high. Therefore, this one-step solid-state reaction method is very successive for synthesizing LiTi_2O_4

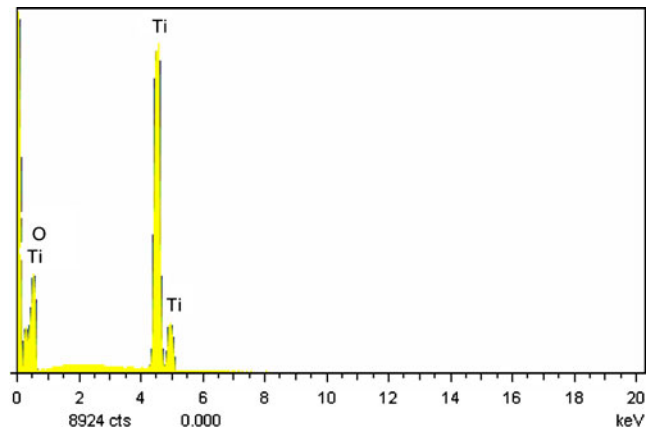


Fig. 2 EDS spectrum of LiTi_2O_4 sample prepared at 850°C for 36 h

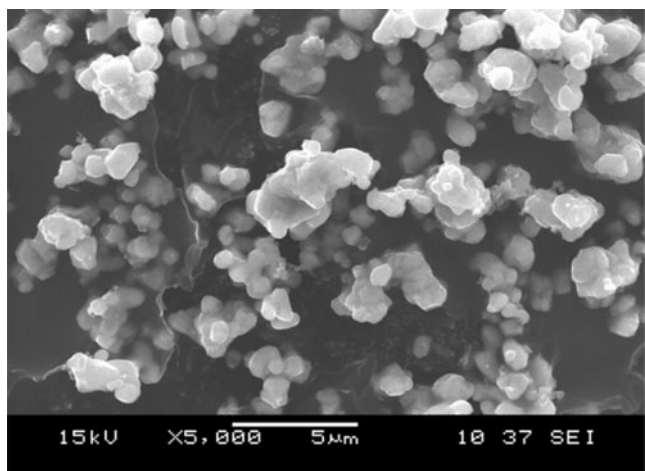


Fig. 3 SEM image of LiTi_2O_4 sample prepared at 850°C for 36 h

electrode material. LiTi_2O_4 electrode is subject to scanning for cyclic voltammetry for 10 times, the result of which is shown in Fig. 5. It is observed that the cyclic peak potentials are stable at about 1.25 and 1.75 V; the average potentials are about 1.50 V and it is in agreement with the reference [24]. The charge quantity of insertion and de-insertion shows slight fading, indicating that LiTi_2O_4 has good reversibility.

LiTi_2O_4 electrode was subject to discharge and charge at 0.2C current rates, and the first results are shown in Fig. 6. It is observed that the operating potential plateaus are extremely flat, indicating that lithium insertion reaction of LiTi_2O_4 transform between the two phases and without any intermediate phase. The discharge capacity is about 133.6 mAh g^{-1} , the charge capacity is about 134.8 mAh g^{-1} , and the average plateau potential is about 1.50 V, which is in agreement with the CV experimental result. LiTi_2O_4

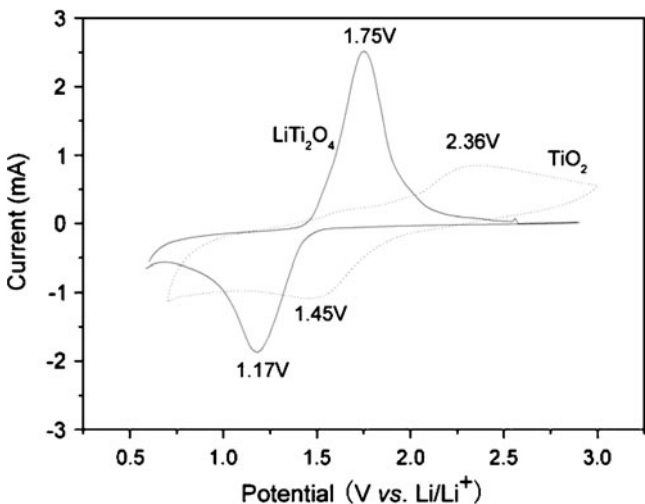


Fig. 4 Cyclic voltammograms of TiO_2 (anatase) and LiTi_2O_4 prepared at 850°C for 36 h in 1 M LiPF_6 /(EC:DMC:EMC) (volume ratio=1:1:1) at 0.5 mV s⁻¹ scan rate

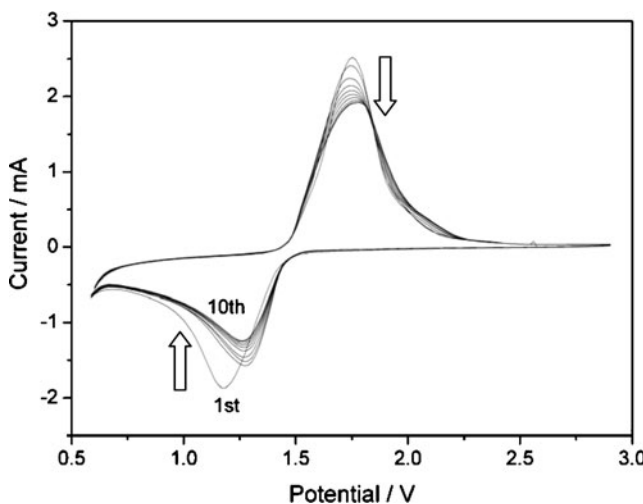


Fig. 5 Voltammetric behavior vs. cycle numbers of LiTi_2O_4 electrode in 1 M LiPF_6 /EC:DMC:EMC (volume ratio=1:1:1) at 0.5 mV s^{-1} scan rate

electrode was subject to cyclic charge and discharge at 0.2, 0.5, and 1.0 C rates for 50 times respectively, and the results of which are shown in Fig. 7. At 0.2 C rate, the 50th discharge capacity is decreased to 130.5 mAh g^{-1} , which is about 97.6% of its initial capacity; at 0.5 C rate, the discharge capacity reduces from 124.1 to 117.1 mAh g^{-1} with a retention of 94.4%; at 1.0 C rate, the discharge capacity decreases from 110.6 to 98.0 mAh g^{-1} ; the columbic efficiency is about 88.6%. This shows that LiTi_2O_4 has good reversibility and high rate performance.

In the process of initial discharge of the $\text{Li/LiTi}_2\text{O}_4$ cell, the electrochemical impedance spectra were determined at different lithium insertion states (3.00, 1.00, and 0.70 V) and the results are given in Fig. 8. At potentials above 1.0 V, the impedance plots are mainly composed of one depressed semicircle and one sloping straight line. The

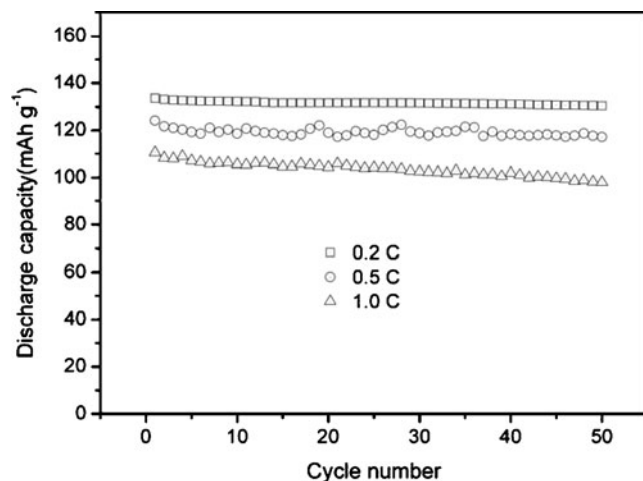


Fig. 7 The specific capacity vs. number of cycle of the $\text{Li/LiTi}_2\text{O}_4$ cell at different current rates: 0.2C, 0.5C, and 1.0C, respectively

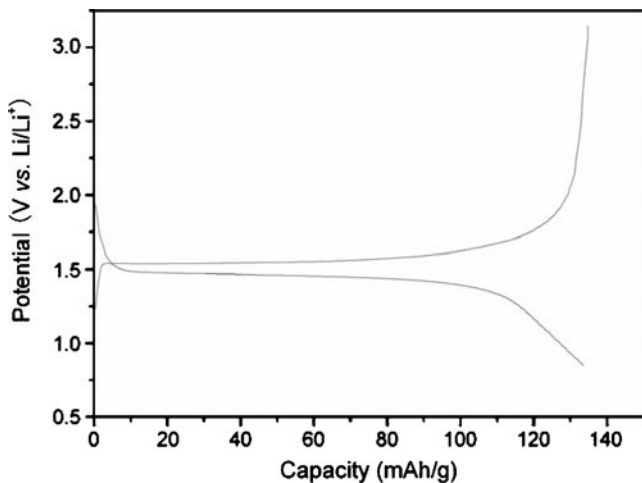


Fig. 6 Initial charge–discharge characteristics of the $\text{Li/LiTi}_2\text{O}_4$ cell at 0.2 C current rate between 3.0 and 0.8 V

semicircles can be considered as due to the electrochemical reaction resistance and the double layer capacitance, and the straight line in the low-frequency range reflects the diffusion of Li^+ ions in the LiTi_2O_4 electrode (Warburg impedance). No semicircle is found in the high-frequency range. It seems that the LiTi_2O_4 electrode is passivation free. It indicates that LiTi_2O_4 anode is much safer for battery operation than either lithium metal or carbonaceous anodes [25]. At 0.70 V, an ambiguous semicircular loop appears in the intermediate-frequency region, it may indicate the occurring phase transition preceding [26]. The details are being investigated in our further work and will be reported later. The ohmic resistance is about $1.8\text{--}2.0 \Omega$, which attributes to the resistance of electrolyte solution, separate film, and electrode. The semicircle corresponding to the charge-transfer procession is influenced by the

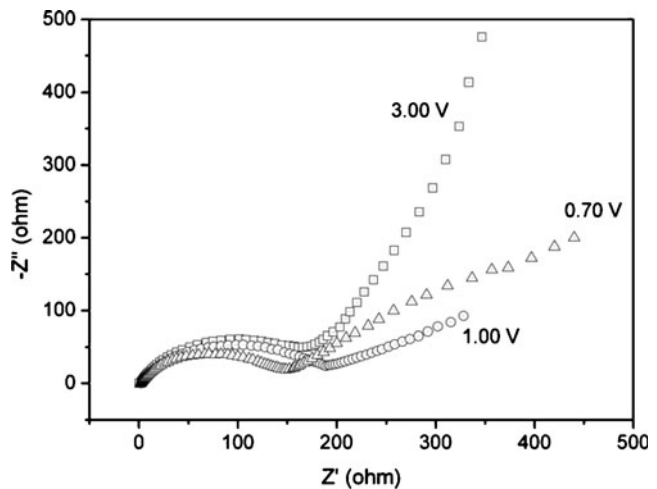


Fig. 8 Nyquist plots of the $\text{Li/LiTi}_2\text{O}_4$ cell at different discharge states of 3.00, 1.00, and 0.70 V, respectively

electrode potential. Such polarization resistance behavior also was observed by Kritil [26].

Conclusions

In this study, a novel method of one-step solid-state reaction was used to synthesize LiTi_2O_4 anode material with carbon black, Li_2CO_3 , and TiO_2 as raw materials. The synthesized LiTi_2O_4 showed pure spinel phase and uniform particle size. In particular, it has good electrochemical reversibility, cyclic stability, and high rate performance. This synthesis method was simple, low cost, and practical, which is expected to make the superconductivity material LiTi_2O_4 into a new type anode material for commercial lithium ion batteries.

Acknowledgments The authors would like to thank the financial support provided by Natural Science Foundation (No: 0679011, 0728215) and the Science and Technology Program (0630004-3A) of Guangxi province in China.

References

- Ohzuku T, Brod RJ (2007) An overview of positive-electrode materials for advanced lithium-ion batteries. *J Power Sources* 174:449–456
- Peramunage D, Abraham KM (1998) The $\text{Li}_4\text{Ti}_5\text{O}_{12}$ //PAN electrolyte// LiMn_2O_4 rechargeable battery with passivation-free electrodes. *J Electrochem Soc* 145:2615–2622
- Colbow KM, Dahn JR, Haering RR (1989) Structure and electrochemistry of the spinel oxides LiTi_2O_4 and $\text{Li}_{4/3}\text{Ti}_{5/3}\text{O}_4$. *J Power Sources* 26:397–402
- Ohzuku T, Ueda A, Yamamoto N (1995) Zero-strain insertion material of $\text{Li}[\text{Li}_{1/3}\text{Ti}_{5/3}]\text{O}_4$ for rechargeable lithium cells. *J Electrochem Soc* 142:1431–1435
- Ariyoshi K, Yamato R, Ohzuku T (2005) Zero-strain insertion mechanism of $\text{Li}[\text{LiTi}]$ O for advanced lithium-ion (shuttlecock) batteries. *Electrochim Acta* 51:1125–1129
- Ronci F, Reale P, Scrosati B, Panero S, Albertini VR, Perfetti P, Michiel MD, Merino JM (2002) High resolution in-situ structural measurements of the $\text{Li}_{4/3}\text{Ti}_{5/3}\text{O}_4$ zero strain insertion material. *J Phys Chem B* 106:3082–3086
- Prosini PP, Mancini R, Petrucci L, Contini V, Villano P (2001) $\text{Li}_4\text{Ti}_5\text{O}_{12}$ as anode in all-solid-state, plastic, lithium-ion batteries for low-power applications. *Solid State Ionics* 144:185–192
- Kuhn A, Baetz C, Garcia-Alvarado F (2007) Structural evolution of ramsdellite-type $\text{Li}_x\text{Ti}_2\text{O}_4$ upon electrochemical lithium insertion–deinsertion ($0 \leq x \leq 2$). *J Power Sources* 174:421–427
- Geng HX, Dong AF, Che GC, Huang WW, Jia SL, Zhao ZX (2005) Investigations on preparation, upper critical field and low temperature thermal expansion of LiTi_2O_4 superconductor. *Physica C* 432:53–58
- Manickam M, Takata M (2003) Lithium intercalation cell $\text{LiMn}_2\text{O}_4/\text{LiTi}_2\text{O}_4$ without metallic lithium. *J Power Sources* 114:298–302
- Sun CP, Lin JY, Mollah S, Ho PL, Yang HD, Hsu FC, Liao YC, Wu MK (2004) Magnetic field dependence of low-temperature specific heat of the spinel oxide superconductor LiTi_2O_4 . *Phys Rev B* 70:54519
- Mergos JA, Dervos CT (2009) Structural and dielectric properties of Li_2O -doped TiO_2 . *Mater Charact* 60:848–857
- Kanno T, Awaka J, Kariya F, Ebisu S, Nagata S (2006) Electrical and magnetic properties of the spinel-type $\text{Li}(\text{Ti}_{0.8}\text{Cr}_{0.2})_2\text{O}_4$. *Physica B* 381:30–33
- Akimoto J, Gotoh Y, Kawaguchi K, Oosawa Y (1992) Preparation of LiTi_2O_4 single crystals with the spinel structure. *J Solid State Chem* 96:446–450
- Chen C, Spears M, Wondre F, Ryan J (2003) Crystal growth and superconductivity of LiTi_2O_4 and $\text{Li}_{1+1/3}\text{Ti}_{2-1/3}\text{O}_4$. *J Cryst Growth* 250:139–145
- Koshiba N, Takata K, Asaka E (1996) Rechargeable lithium cell and process for making an anode for use in the cell. US Patent 5,545,468 13 Aug. 1996
- Jiang K, Hu XH, Sun HJ, Wang DH, Jin XB, Ren YY, Chen GZ (2004) Electrochemical synthesis of LiTiO_2 and LiTi_2O_4 in molten LiCl . *Chem Mater* 16:4324–4329
- Murphy DW, Cava RJ, Zahurak SM, Santoro A (1983) Ternary Li_xTiO_2 phases from insertion reactions. *Solid State Ionics* 9–10:413–418
- Cava RJ, Murphy DW, Zahurak S, Santoro A, Roth RS (1984) The crystal structures of the lithium-inserted oxides $\text{Li}_{0.5}\text{TiO}_2$ anatase, LiTi_2O_4 spinel, and $\text{Li}_2\text{Ti}_2\text{O}_4$. *J Solid State Chem* 50 (1):64–75
- Fattakhova D, Petrykin V, Brus J, Kostlánová T, Dědeček J, Krtík P (2005) Solvothermal synthesis and electrochemical behavior of nanocrystalline cubic Li–Ti–O oxides with cationic disorder. *Solid State Ionics* 176(23–24):1877–1885
- Persi L, Croce F, Scrosati B (2002) A LiTi_2O_4 – LiFePO_4 novel lithium-ion polymer battery. *Electrochim Commun* 4:92–95
- Zhu CG, Zhou XF, Chu DB (2003) Electrolytic preparation of nanograde LiTi_2O_4 powder. *Fine Chemical Industry* 4:244–246
- Cai ZP, Liang Y, Li WS, Xing LD, Liao YH (2009) Preparation and performances of LiFePO_4 cathode in aqueous solvent with polyacrylic acid as a binder. *J Power Sources* 189:547–551
- Kuhn A, Amandi R, Garcia-Alvarado F (2001) Electrochemical lithium insertion in TiO_2 with the ramsdellite structure. *J Power Sources* 92:221–227
- Wang GX, Bradhurst DH, Dou SX, Liu HK (1999) Spinel $\text{Li}[\text{Li}_{1/3}\text{Ti}_{5/3}]\text{O}_4$ as an anode material for lithium ion batteries. *J Power Sources* 83:156–161
- Krtík P, Fattakhova D (2001) Li insertion into Li–Ti–O spinels: voltammetric and electrochemical impedance spectroscopy study. *J Electrochem Soc* 148(9):A1045–A1050